Mon. Not. R. Astron. Soc. **411,** 2099–2112 (2011) doi:10.1111/j.1365-2966.2010.17848.x

Investigating coronal saturation and supersaturation in fast-rotating M-dwarf stars

R. D. Jeffries,[1⋆] R. J. Jackson,[1] K. R. Briggs,[2] P. A. Evans[3] and J. P. Pye[3]

[1]*Astrophysics Group, Research Institute for the Environment, Physical Sciences and Applied Mathematics, Keele University, Staffordshire ST5 5BG*
[2]*ETH Zurich, Institute of Astronomy, 8093 Zurich, Switzerland*
[3]*Department of Physics and Astronomy, University of Leicester, University Road, Leicester LE1 7RH*

Accepted 2010 October 11. Received 2010 October 8; in original form 2010 August 3

ABSTRACT

At fast rotation rates, the coronal activity of G- and K-type stars has been observed to 'saturate' and then decline again at even faster rotation rates – a phenomenon dubbed 'supersaturation'. In this paper, we investigate coronal activity in fast-rotating M-dwarfs using deep *XMM–Newton* observations of 97 low-mass stars of known rotation period in the young open cluster NGC 2547 and combine these with published X-ray surveys of low-mass field and cluster stars of known rotation period. Like G- and K-dwarfs, we find that M-dwarfs exhibit increasing coronal activity with decreasing Rossby number $N_{\rm R}$, the ratio of period to convective turnover time, and that activity saturates at $L_{\rm X}/L_{\rm bol} \simeq 10^{-3}$ for $\log N_{\rm R} < -0.8$. However, supersaturation is not convincingly displayed by M-dwarfs, despite the presence of many objects in our sample with $\log N_{\rm R} < -1.8$, where supersaturation is observed to occur in higher mass stars. Instead, it appears that a short rotation period is the primary predictor of supersaturation; $P \leq 0.3$ d for K-dwarfs and perhaps $P \leq 0.2$ d for M-dwarfs. These observations favour the 'centrifugal stripping' model for supersaturation, where coronal structures are forced open or become radiatively unstable as the Keplerian corotation radius moves inside the X-ray-emitting coronal volume.

Key words: stars: activity – stars: coronae – stars: rotation – open clusters and associations: individual: NGC 2547 – X-rays: stars.

1 INTRODUCTION

X-ray emission from the hot coronae of photospherically cool stars arises from magnetically confined and heated plasma with temperatures in excess of 10^6 K (see the review by Güdel 2004). X-ray observations of cool stars with convective envelopes have long since shown that X-ray activity increases with the rotation rate and has led to the paradigm that a magnetic dynamo process produces and maintains the required magnetic fields, in analogy to processes observed to occur in the Sun (e.g. Pallavicini et al. 1981; Mangeney & Praderie 1984). The influence of a regenerative dynamo is supported by observations of coronal activity in stars at a range of masses. These demonstrate, in accordance with expectations from dynamo models, that rotation is not the only important parameter. The best correlations are found between increasing magnetic activity and the inverse of the Rossby number (e.g. Noyes et al. 1984; Dobson & Radick 1989; Pizzolato et al. 2003), where the Rossby number is $P/\tau_{\rm c}$, the ratio of the stellar rotation period, P, to the convective turnover time, $\tau_{\rm c}$. According to stellar models, $\tau_{\rm c}$ increases towards lower masses (e.g. Gilliland 1986; Kim & Demarque 1996) and hence, for a given rotation period, a K-dwarf has a smaller Rossby number and is more magnetically active than a G-dwarf, where magnetic activity is expressed in a form normalized by the bolometric luminosity (e.g. the ratio of coronal X-ray to bolometric luminosity, $L_{\rm X}/L_{\rm bol}$).

Many young, cool stars have not lost significant angular momentum and rotate much more rapidly than the Sun, leading to higher coronal X-ray luminosities by several orders of magnitude. At fast rotation rates, magnetic activity (as measured in the corona and chromosphere) appears to 'saturate' (e.g. Vilhu & Walter 1987; Stauffer et al. 1994). Saturated coronal activity is manifested as a plateau of $L_{\rm X}/L_{\rm bol} \simeq 10^{-3}$ in G-dwarfs with rotation periods less than about 3 d. In lower mass stars, the plateau in coronal activity is at a similar level but the rotation period at which it first occurs is longer. A unified picture emerges by plotting X-ray activity against the Rossby number (Stępień 1994; Patten & Simon 1996; Randich et al. 1996; Pizzolato et al. 2003), such that coronal saturation occurs at Rossby numbers of about 0.1 in stars of spectral types G, K and M. This unification in terms of a parameter associated with dynamo efficiency suggests that coronal saturation reflects a saturation of the dynamo itself (Vilhu & Walter 1987), although other

⋆E-mail: rdj@astro.keele.ac.uk

explanations, such as a redistribution of radiative losses to other wavelengths (Doyle 1996) or changes in magnetic topology with fast rotation (Solanki, Motamen & Keppens 1997; Jardine & Unruh 1999; Ryan, Neukirch & Jardine 2005), must also be considered.

At rotation rates approximately five times faster than required for saturation, it appears that coronal activity turns down again – a phenomenon dubbed 'supersaturation' (Prosser et al. 1996). Examples of supersaturated G- and K-stars, with $L_{\rm X}/L_{\rm bol} \simeq 10^{-3.5}$, have been found in a number of young open clusters (Stauffer et al. 1994, 1997; Patten & Simon 1996; Randich 1998; Jeffries et al. 2006), among the fast-rotating components of contact W UMa binaries (Cruddace & Dupree 1984; Stępień, Schmitt & Voges 2001), and have been suggested as the reason for lower X-ray activity in the fastest-rotating, very young pre-main-sequence (PMS) stars (Stassun et al. 2004; Preibisch et al. 2005; Dahm et al. 2007). Possible explanations for coronal supersaturation include negative feedback in the dynamo (Kitchatinov, Rüdiger & Küker 1994), decreasing coverage by active regions (Stępień et al. 2001), reorganization of the coronal magnetic field (Solanki et al. 1997) or centrifugal stripping of the corona (Jardine 2004).

An important test of these ideas is to look at the coronal properties of fast rotators across a wide range of masses. In particular, it is vital to gauge whether saturation and supersaturation occur at fixed values of the rotation period or Rossby number. This would illuminate which physical mechanisms are responsible. One of the principal gaps in our knowledge is the behaviour of coronal emission for ultra-fast rotating M-dwarfs. These have larger convection zones (as a fraction of the star), longer convective turnover times and hence smaller Rossby numbers at a given rotation period than G- and K-dwarfs. Of course M-dwarfs also have much lower bolometric luminosities than G- or K-dwarfs and so, at a given magnetic activity level, they are harder to observe in the young open clusters where the majority of ultra-fast rotators are found.

The most comprehensive work so far was by James et al. (2000) using X-ray observations for a small, inhomogeneous sample of fast-rotating low-mass stars from the field and open clusters. They found that, like G- and K-type stars, M-dwarfs with periods below $\sim$6 d and Rossby numbers below 0.1 showed saturated levels of X-ray emission with $L_{\rm X}/L_{\rm bol} \simeq 10^{-3}$. They also claimed tentative evidence for supersaturation in the fastest-rotating M-dwarfs with periods of 0.2–0.3 d.

In this paper, we re-visit the question of saturation and supersaturation of coronal emission in fast-rotating M-dwarfs. We analyse new, deep *XMM–Newton* observations of a large, homogeneous sample of rapidly-rotating M-dwarfs identified in the open cluster NGC 2547 by Irwin et al. (2008). NGC 2547 has an age of 35–38 Myr (Jeffries & Oliveira 2005; Naylor & Jeffries 2006) and a rich population of low-mass stars (Jeffries et al. 2004). However, the cluster is at $\sim$400 pc and while previous X-ray observations with *ROSAT* (Jeffries & Tolley 1998) and *XMM–Newton* (Jeffries et al. 2006) demonstrated an X-ray-active low-mass population, they were insufficiently sensitive to probe the coronal activity of its M-dwarfs in any detail.

In Section 2, we describe the new *XMM–Newton* observations of NGC 2547 and the identification of X-ray sources with rapidly-rotating M-dwarfs from the Irwin et al. (2008) catalogue. In Section 3, we combine X-ray and optical data, estimate coronal activity levels and examine the evidence for coronal saturation and supersaturation, using a homogeneous sample of fast-rotating M-dwarfs, several times larger than considered by James et al. (2000). In Section 4, we compare our results to those compiled in the literature for G- and K-stars and for other samples of M-dwarfs. In Section 5, we discuss our results in the context of competing models for saturation/supersaturation and our conclusions are summarized in Section 6.

2 *XMM–NEWTON* OBSERVATIONS OF NGC 2547

NGC 2547 was observed with *XMM–Newton* between UT 22:30:03 on 2007 November 12 and UT 09:30:03 on 2007 November 14 using the European Photon Imaging Counter (EPIC) instrument, for a nominal exposure time of 125.8 ks (Observation ID 0501790101). The two EPIC-MOS cameras and the EPIC-PN camera were operated in full-frame mode (Strüder et al. 2001; Turner et al. 2001), using the medium filter to reject optical light. The nominal pointing position of the observation was RA $= 08^{\rm h}\,10^{\rm m}\,06\overset{\rm s}{.}1$, Dec. $= -49^{\circ}\,15'\,42\overset{''}{.}9$ (J2000.0).

2.1 Source detection

Version 7.1 of the *XMM–Newton* SAS (Science Analysis System) was used for the initial data reduction and source detection. Data from the three cameras were individually screened for high background periods and these time-intervals were excluded from all subsequent analyses. Observation intervals were excluded where the total count rate for events with energies >10 keV exceeded 0.35 and 1.0 $\rm s^{-1}$ for the MOS and PN detectors, respectively. The remaining useful exposure times were 107.3, 104.8 and 87.4 ks for the MOS1, MOS2 and PN cameras, respectively, which can be compared with the equivalent exposure times of 29.0, 29.4 and 13.6 ks in the less-sensitive observation analysed by Jeffries et al. (2006).

Images were created using the EVSELECT task and a spatial sampling of 2 arcsec $\rm pixel^{-1}$. The event lists were filtered to exclude anomalous pixel patterns and edge effects by including only those events with 'pattern' $\leq$12 for the MOS detectors and $\leq$4 for the PN detectors. The contrast between background and source events was also increased by retaining only those events in channels corresponding to energies of 0.3–3 keV.

The EDETECT_CHAIN task was used to find sources with a combined maximum log-likelihood value greater than 10 (approximately equivalent to $-\ln p$, where p is the probability that the 'source' is due to a background fluctuation), in all three instruments combined, over the 0.3–3 keV energy range. We expect one to two spurious X-ray detections at this level of significance, though they would be highly unlikely to correlate with NGC 2547 members, so will not hamper any analysis in this paper. The individual images from each instrument were source-searched first to confirm there were no systematic differences in the astrometry of the brightest sources. Count rates in each detector were determined using vignetting-corrected exposure maps created within the same task. In addition, count rates were determined for each source in the 0.3–1.0 and 1.0–3.0 keV bands separately, in order to form a hardness ratio (HR). A total of 323 significant X-ray sources were found. Some of these only have count rates measured in a subset of the three instruments, because they fell in gaps between detectors, on hot pixels or lay outside the field of view. In addition, we decided only to retain count rates for analysis, if they had a signal-to-noise ratio greater than 3, which resulted in the removal of three sources from our list.

To check the EPIC astrometric solution, we cross-correlated all the brightest X-ray sources (those detected with a maximum log likelihood greater than 100) against a list of photometrically selected NGC 2547 members compiled by Naylor et al. (2002, their table 6), which is based on D'Antona & Mazzitelli (1997) isochrones

and *BVI* photometry and which incorporates bright cluster members from Clariá (1982). There were 98 correlations found within 6 arcsec of the nominal X-ray position and as discussed in Jeffries et al. (2006), where a similar procedure was followed, these correlations are very likely to be the genuine optical counterparts of the X-ray sources. The mean offset between the X-ray and optical positions was 0.11 arcsec in RA and 0.59 arcsec in Dec. As the optical catalogues have an absolute accuracy better than 0.2 arcsec and an internal precision of about 0.05 arcsec, the X-ray positions were corrected for these offsets. The remaining dispersion in the offsets indicates an additional 1 arcsec uncertainty (in addition to the quoted astrometric uncertainty from the source-searching routines) in the X-ray positions, concurring with the current astrometric calibration assessment of the *XMM–Newton* science operations centre (Guainazzi 2010).

2.2 Cross-correlation with the Irwin catalogue

The purpose of this paper is to study the properties of fast-rotating M-dwarfs, so an investigation of the full X-ray source population is deferred to a later paper. Here, we discuss cross-correlations between the astrometrically corrected X-ray source list and the catalogue of cool stars with known rotation periods in NGC 2547, given by Irwin et al. (2008). The Irwin et al. (2008) catalogue contains precise positions tied to the 2MASS reference frame, rotation periods and photometry in the V and I bands. We found significant systematic differences (of up to 0.2 mag) between the photometry of Irwin et al. (2008) and that found in Naylor et al. (2002) for stars common to both. As the accuracy of the Naylor et al. photometry has support from an independent study by Lyra et al. (2006), we transformed the Irwin photometry using the following best-fitting relationships between the Naylor et al. and Irwin et al. photometry:

$$V = 1.029\,V_{\rm Irwin} - 0.428 \qquad {\rm rms} = 0.08\,{\rm mag}, \tag{1}$$

$$V - I = 1.177\,(V - I)_{\rm Irwin} - 0.305 \qquad {\rm rms} = 0.10\,{\rm mag}, \tag{2}$$

where the calibrations transform the photometry on to the Johnson–Cousins calibration used by Naylor et al. and are valid for $14 < V < 21$ and $1.2 < (V - I) < 3.4$. We take the rms deviation from these relationships as the photometric uncertainty in subsequent analysis.

A maximum correlation radius between X-ray and optical sources of 5 arcsec resulted in 68 correlations from the 97 Irwin et al. (2008) objects that are within the EPIC field of view (there were no correlations between 5-arcsec and our nominal 6-arcsec acceptance threshold). The missing objects were predominantly the optically faintest (see Section 3.2). Experiments involving offsetting the X-ray source positions by 30 arcsec in random directions suggest that fewer than one of these correlations would be expected by chance. The details of the correlations along with count rates, HRs and correlation separations appear in Table 1 (available fully in electronic form only).

2.3 Fluxes and coronal activity

To assess magnetic activity levels, X-ray count rates were converted into fluxes using a single conversion factor for each instrument. The use of a single conversion factor is necessitated because few of the X-ray sources that correlate with the Irwin et al. (2008) sample have sufficient counts (>500) to justify fitting a complex spectral model. The median source is detected in the EPIC-PN camera with about 150 counts and a signal-to-noise ratio of only 10. Instead,

Table 1. : X-ray detections of sources in the Irwin et al. (2008) catalogue of NGC 2547 members with rotation periods. The table is available electronically (see Supporting Information) and contains 69 rows. Only two rows are shown here as a guide to the form and content. Columns are as follows: (1) – Identification from Irwin et al. (2008); (2) and (3) – RA and Dec. (J2000.0, from Irwin et al. 2008); (4) and (5) – V and $V - I$ magnitudes (modified from the Irwin et al. 2008 values – see Section 2.2); (6) – rotation period (from Irwin et al. 2008); (7) – V-band bolometric correction (see Section 2.3); (8) −log bolometric luminosity (assuming a distance of 400 pc); (9) −log convective turnover time (see equation 3); (10) – log Rossby number; (11) and (12) – stellar mass and radius (estimated from the Siess, Dufour & Forestini 2000 models); (13) – Keplerian corotation radius as a multiple of the stellar radius; (14) and (15) – RA and Dec. of the X-ray source; (16) – the maximum log likelihood of the detection; (17) – separation from the optical counterpart; (18) and (19) – total PN count rate (0.3–3 keV); (20) and (21) – PN count rate (0.3–1 keV, the '*S*' band); (22) and (23) – PN count rate (1–3 keV, the '*H*' band); (24) and (25) – PN HR [defined as $(H - S)/(H + S)$]; (26) and (27) – total MOS1 count rate (0.3–3 keV); (28) and (29) – total MOS2 count rate (0.3–3 keV); (30) and (31) – X-ray flux (0.3–3 keV); (32) and (33) – log X-ray to bolometric flux ratio; and (34) and (35) – cross-identification with Naylor et al. (2002) where available.

Name	RA (J2000)	Dec,	V	$V - I$	P (d)	BC	$\log L_{\rm bol}/{\rm L}_\odot$	$\log \tau_{\rm c}$ (d)	$\log N_{\rm R}$	$M/{\rm M}_\odot$	$R/{\rm R}_\odot$	$R_{\rm Kepler}/R$
(1)	(2)	(3)	(4)	(5)	(6)	(7)	(8)	(9)	(10)	(11)	(12)	(13)
N2547-1-5-417	8 09 25.91	−49 09 58.4	18.69	2.80	0.865	−2.28	−1.40	1.80	−1.86	0.37	0.47	5.76
N2547-1-5-1123	8 09 17.71	−49 08 34.5	19.57	3.16	0.413	−2.76	−1.56	1.88	−2.26	0.28	0.42	3.62

X-ray RA	X-ray Dec.	ML	Sep	PN0	PN0_err	PN1	PN1_err	PN2	PN2_err	HR	HR_err
(°, J2000.0)			(arcsec)	(s^{-1}, 0.3–3 keV)		(s^{-1}, 0.3–1 keV)		(s^{-1}, 1–3 keV)			
(14)	(15)	(16)	(17)	(18)	(19)	(20)	(21)	(22)	(23)	(24)	(25)
122.35782	−49.1664	421.1	0.62	7.23e−03	5.23e−04	5.00e−03	4.21e−04	2.23e−03	3.11e−04	−0.38	0.07
122.32372	−49.1431	36.4	0.57	1.84e−03	3.76e−04	1.33e−03	2.99e−04	5.04e−04	2.28e−04	−0.45	0.20

MOS1	MOS1_err	MOS2	MOS2_err	Flux	Flux_err	$\log L_{\rm X}/L_{\rm bol}$	$\Delta\log L_{\rm X}/L_{\rm bol}$	Naylor ID	
(s^{-1}, 0.3–3 keV)		(s^{-1}, 0.3–3 keV)		(erg cm s^{-1}, 0.3–3 keV)					
(26)	(27)	(28)	(29)	(30)	(31)	(32)	(33)	(34)	(35)
1.82e−03	2.41e−04	1.80e−03	2.32e−04	9.59e−15	9.87e−16	−2.92	0.08	14	1171
4.85e−04	1.62e−04	5.47e−04	1.82e−04	2.80e−15	6.05e−16	−3.30	0.12	4	2832

we designed a spectral model that agrees with the mean HR in the EPIC-PN camera, defined as $(H - S)/(H + S)$, where S is the 0.3–1.0 keV count rate and H is the 1.0–3.0 keV count rate.

Our starting point was the analysis of an earlier, much shorter *XMM–Newton* observation of NGC 2547 (Jeffries et al. 2006). This showed that single-temperature thermal plasma models were insufficiently complex to fit the spectra of active stars in NGC 2547. A two-temperature 'MEKAL' model (Mewe, Kaastra & Leidahl 1995) provided a satisfactory description, with $T_1 \simeq 0.6$ keV, $T_2 \simeq 1.5$ keV and an emission measure ratio (hot/cool) of about 0.7, which was chosen to approximately match the mean HR. This crude approximation to the differential emission measure (DEM) of the coronal plasma reasonably matches detailed work on the coronal DEM of several nearby, rapidly rotating low-mass stars, which show a DEM maximum at around 10^7 K (García-Alvarez et al. 2008). It was also established in Jeffries et al. (2006) that the coronal plasma was best fitted with a subsolar metallicity ($Z \simeq 0.3$), which seems to be a common feature for very active stars, including fast-rotating K- and M-dwarfs (e.g. Briggs & Pye 2003; García-Alvarez et al. 2008).

Adopting the same model, we have used the software package XSPEC and instrument response files appropriate for the EPIC-PN camera at the time of the observations to calculate a conversion factor from 0.3–3.0 keV count rates to an *unabsorbed* 0.3–3.0 keV flux. We assumed an interstellar absorbing column density of neutral hydrogen $N_{\rm H} = 3 \times 10^{20}$ cm^{-2} (see Section 2.5). The derived flux conversion factor is 1.68×10^{-12} erg cm^{-2} per count and the derived HR is -0.42, which closely matches the mean HR in our sample (see Section 3). Analogous conversion factors for the EPIC-MOS cameras were derived by dividing the EPIC-PN conversion factor by the weighted mean ratio of the observed MOS and PN count rates. This gave conversion factors of 6.22×10^{-12} erg cm^{-2} per count for both of the EPIC-MOS cameras.

The unabsorbed 0.3–3 keV X-ray flux for each detected Irwin et al. (2008) star is found from a weighted average of fluxes from each detector. Uncertainties in these fluxes arise from the count rate errors, but we added a further 10 per cent systematic error in quadrature to each detector count rate to account for uncertainties in the instrument response and in the the point spread function modelling in the EDETECT_CHAIN task (e.g. Saxton 2003; Guainazzi 2010). From the average fluxes, the coronal activity indicator $L_{\rm X}/L_{\rm bol}$ was calculated by using the corrected V magnitudes, an extinction $A_V = 0.19$, a reddening $E(V - I) = 0.077$ (see Clariá 1982; Naylor et al. 2002) and the relationship between intrinsic $V - I$ and bolometric correction described by Naylor et al. (2002). For the red stars in our sample with $V - I > 1.5$, these bolometric corrections are based on the empirical measurements of Leggett et al. (1996). The bolometric corrections and $L_{\rm X}/L_{\rm bol}$ values are reported in Table 1.

2.4 Flux upper limits

There are 29 objects in the Irwin et al. (2008) catalogue within the *XMM–Newton* field of view (for only a subset of the detectors in some cases), but not found as sources by the EDETECT_CHAIN task. We inspected the X-ray images at the positions of these sources and found one example (N2547-1-6-5108), which is a reasonably bright X-ray source, that appears only in the MOS2 image, and which was missed by the automated source searching. We evaluated the X-ray count rates for this object using a 20-arcsec-radius aperture (see below) and a local estimate of the background. This source has been added to Table 1. There were no X-ray sources apparent at the positions of the other 28 objects and X-ray flux upper limits were derived as follows. In the EDETECT_CHAIN task, we generated images for each detector consisting of smooth models of the X-ray background, to which were added *models* of the significantly detected sources calculated from their count rates and the model point spread function used to detect and parametrize them. These images were 'noise-free' estimates of the expected X-ray background for any given position. The total expected background was summed within circles of radius 20 arcsec surrounding each of the undetected Irwin et al. (2008) objects. The number of observed X-ray counts in those areas in the original X-ray images was also summed, consisting of both source and background counts. A 3σ upper limit to the number of source counts was calculated using the Bayesian approach formulated by Kraft, Burrows & Nousek (1991). The choice of a 20 arcsec radius follows the work of Carrera et al. (2007), who showed that 'aperture photometry' using this radius gave count rates that closely matched those found in EDETECT_CHAIN. The upper limits to the X-ray count *rates* were determined by dividing by the average exposure time within the same circular area.

Using this technique, we found that where objects were covered by both PN and MOS data, the PN data were at least a factor of 2 more sensitive. Rather than attempting to combine the results from the three instruments, we have either (i) taken the upper limit from the PN, where PN data are present (23 objects); (ii) taken the upper limit from one MOS detector where an object was only covered by that detector (three objects); or (iii) taken the average upper limit from both MOS detectors (two objects) and divided by $\sqrt{2}$, as in these cases, the two upper limits were very similar. The count-rate upper limits were converted to upper limits in X-ray flux and upper limits to $L_{\rm X}/L_{\rm bol}$ using the procedures described in the previous subsection. The details of the upper limit measurements are presented separately in Table 2 (available in electronic form only).

2.5 Uncertainties in X-ray fluxes

The uncertainties in the $\log L_{\rm X}/L_{\rm bol}$ values quoted in Table 1 incorporate the statistical count-rate uncertainties and the systematic instrument response uncertainties mentioned in Section 2.3. In addition, we have included (in quadrature) uncertainties in the bolometric flux due to the photometric uncertainties (or variability) implied by equations (1) and (2), which amount to about ± 0.07 dex. The final quoted uncertainties range from 0.08 to 0.21 dex, with a mean of 0.10 dex.

Other contributing uncertainties have also been considered. The X-ray flux conversion factors are rather insensitive to the details of the spectral model. For instance, doubling the temperature of the hot component increases the conversion factor by just 3 per cent and the HR increases to -0.39; varying the metal abundance in the range $0.1 < Z < 1.0$ changes the conversion factor by only ± 5 per cent; and doubling the ratio of hot to cool plasma emission measures increases the conversion factor by 3 per cent and increases the HR to -0.32. The value assumed for $N_{\rm H}$ has a little more effect. The value of $N_{\rm H} = 3 \times 10^{20}$ cm^{-2} is derived from the cluster reddening of $E(B - V) = 0.06 \pm 0.02$ (Clariá 1982), and the relationship between reddening and $N_{\rm H}$ found by Bohlin, Savage & Drake (1978), and could be uncertain by factors of 2. Altering $N_{\rm H}$ from our assumed value to either 1.5×10^{20} or 6×10^{20} cm^{-2} would lead to conversion factors about 5 per cent smaller or 10 per cent larger and HR would change to either -0.44 or -0.35, respectively. All these uncertainties are small compared with those we have already considered and they are neglected.

Table 2. The properties of stars from the Irwin et al. (2008) catalogue that have known rotation periods but were not detected within the *XMM–Newton* field. The table is available electronically (see Supporting Information) and contains 28 rows. Only two rows are shown here as a guide to the form and content. The first 13 columns contain the same properties as listed in Table 1; following these, column (14) lists a flag denoting from which *XMM–Newton* instrument the X-ray count-rate upper limit was derived: 'P' for the PN, 'M1' for MOS1, 'M2' for MOS2 and 'M12' for the average from MOS1 and MOS2 (see text for details). Column (15) lists the 3σ count-rate upper limit in that instrument, column (16) lists the corresponding flux upper limit (0.3–3 keV) and column (17) lists the $\log L_{\rm X}/L_{\rm bol}$ upper limit. Columns (18) and (19) list the cross-identification with the Naylor et al. (2002) catalogue where available.

Name	RA	Dec. (J2000)	V	$V-I$	P (d)	BC	$\log L_{\rm bol}/{\rm L}_\odot$	$\log \tau_{\rm c}$ (d)	$\log N_{\rm R}$	$M/{\rm M}_\odot$	$R/{\rm R}_\odot$	$R_{\rm Kepler}/R$
(1)	(2)	(3)	(4)	(5)	(6)	(7)	(8)	(9)	(10)	(11)	(12)	(13)
N2547-1-5-3742	8 09 25.73	−49 03 15.7	19.16	2.92	0.807	−2.43	−1.53	1.86	−1.96	0.30	0.43	5.64
N2547-1-6-2487	8 10 04.56	−49 06 04.2	14.26	1.00	5.488	−0.27	−0.43	1.31	−0.57	0.88	0.85	14.76

Instrument	Upper limit (s^{-1})	Flux (erg cm s^{-1}, 0.3–3 keV)	$\log L_{\rm X}/L_{\rm bol}$	Naylor ID	
(14)	(15)	(16)	(17)	(18)	(19)
P	<5.20e−03	<8.73e−15	<−2.84	4	1258
P	<1.16e−03	<1.96e−15	<−4.59	3	760

The final source of uncertainty is difficult to quantify, but is probably dominant when considering a single epoch of X-ray data, namely the coronal variability of active stars. Active, low-mass stars show frequent X-ray-flaring behaviour on time-scales of minutes and hours, resulting in an upward bias in an X-ray flux estimated, as here, over the course of more than a day. The more active the low-mass star is, the more frequently it exhibits large X-ray flares (Audard et al. 2000). Rather than trying to correct for this, and as the comparison samples in Section 4 have not had any flare exclusion applied, we continue to use the time-averaged X-ray flux to represent coronal activity. An idea of the uncertainties can be gained by looking at similar estimates from more than one epoch. For example, Gagné, Caillault & Stauffer (1995) find that young Pleiades low-mass stars show differences of more than a factor of 2 in their X-ray fluxes only 25 per cent of the time on time-scales of 1–10 yr. Marino et al. (2003) find that the median level of X-ray flux variability of K3-M dwarfs in the Pleiades is about 0.2 dex on time-scales of months. Jeffries et al. (2006) looked at the variability of G- to M-dwarfs in NGC 2547 itself on time-scales of 7 yr, finding a median absolute deviation from equal X-ray luminosity of about 0.1 dex in G- and K-dwarfs, with a hint that the M-dwarfs are slightly more variable. Only about 20 per cent of sources varied by more than a factor of 2. Our conclusion is that we should assume an additional uncertainty of about 0.1–0.2 dex in our single-epoch measurements, but we caution that the distribution is probably non-Gaussian in the sense that a sample will probably contain a small number of objects that are upwardly biased by more than a factor of 2 by large flares.

3 CORONAL ACTIVITY IN THE M-DWARFS OF NGC 2547

3.1 Hardness ratios

In Fig. 1, we show the dependence of the HR, measured by the PN camera, on the intrinsic colour of the star and on the magnetic activity level, expressed as $L_{\rm X}/L_{\rm bol}$. There is no significant dependence of HR on colour and hence the approximation of a uniform flux conversion factor with spectral type is shown to be reasonable. The weighted mean HR is -0.42 ± 0.02, with a standard deviation of 0.16. The standard deviation is about twice that expected from the statistical errors, hinting at some genuine HR variation. Note that this assumes that the HR uncertainties are symmetric and Gaussian, even though the X-ray data are Poissonian in nature and the HR is strictly limited to $-1 \leq {\rm HR} \leq 1$ (e.g. see Park et al. 2006). The majority of sources are detected with sufficiently large numbers of counts in both energy ranges and with sufficiently precise count rates to make such an assumption reasonable. The second plot shows there is some evidence that the HR increases slightly with the activity level. A best-fitting linear model is ${\rm HR} = -0.09(\pm0.12) + 0.11(\pm0.04)\log L_{\rm X}/L_{\rm bol}$, but the residuals suggest there may still be star-to-star variation at a given activity level. Note though that time-variability of the X-ray activity or HR values has not been considered (see Section 2.5) and this might plausibly account for some of this star-to-star variation.

A significant increase in average coronal temperatures (and hence HR) with activity level is well established in field stars (e.g. Telleschi et al. 2005). The relationship between the HR and $L_{\rm X}/L_{\rm bol}$ found here and the size of the intrinsic scatter are indistinguishable from those found for somewhat higher mass G- and K-stars in NGC 2547 by Jeffries et al. (2006), as is the likelihood of an intrinsic scatter. The mean HR agrees well (by design) with the HR predicted by the spectral model used to calculate the X-ray fluxes. The probable intrinsic variation in the HR at a given $L_{\rm X}/L_{\rm bol}$ corresponds to variations of about a factor of 2 in the emission measure ratio of the hot and cool plasmas in the two-temperature coronal model. Such variations lead to very small uncertainties in $L_{\rm X}/L_{\rm bol}$ of the order a few per cent (see Section 2.5) and so we have not attempted to correct for them.

3.2 X-ray activity

Fig. 2(a) shows a V versus $V-I$ colour–magnitude diagram for the stars of the Irwin et al. (2008) sample (with rotation periods), which lie within the *XMM–Newton* field of view. As a comparison, we show photometric members of NGC 2547 (from Naylor et al. 2002) that also lie within the X-ray field of view and indicate those which have an X-ray counterpart among the 323 significant X-ray sources reported in Section 2.1. Fig. 2(a) shows that the Irwin et al. (2008) sample is only about 50 per cent complete. A significant fraction of photometic cluster candidates at all colours have no detected rotation periods. Most of these non-periodic candidates are X-ray

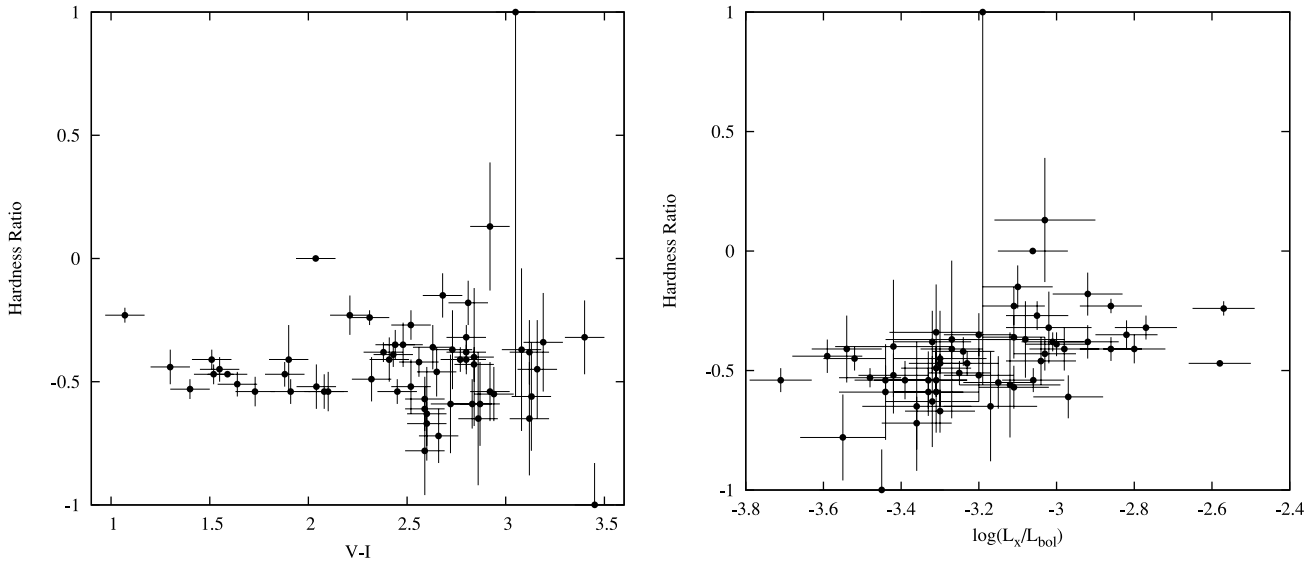

Figure 1. HRs for the NGC 2547 sample [defined as $(H - S)/(H + S)$, where H is the 1.0–3.0 keV count rate and S is the 0.3–1.0 keV count rate in the EPIC-PN camera] as a function of (a) $V - I$ colour and (b) the X-ray-to-bolometric flux ratio.

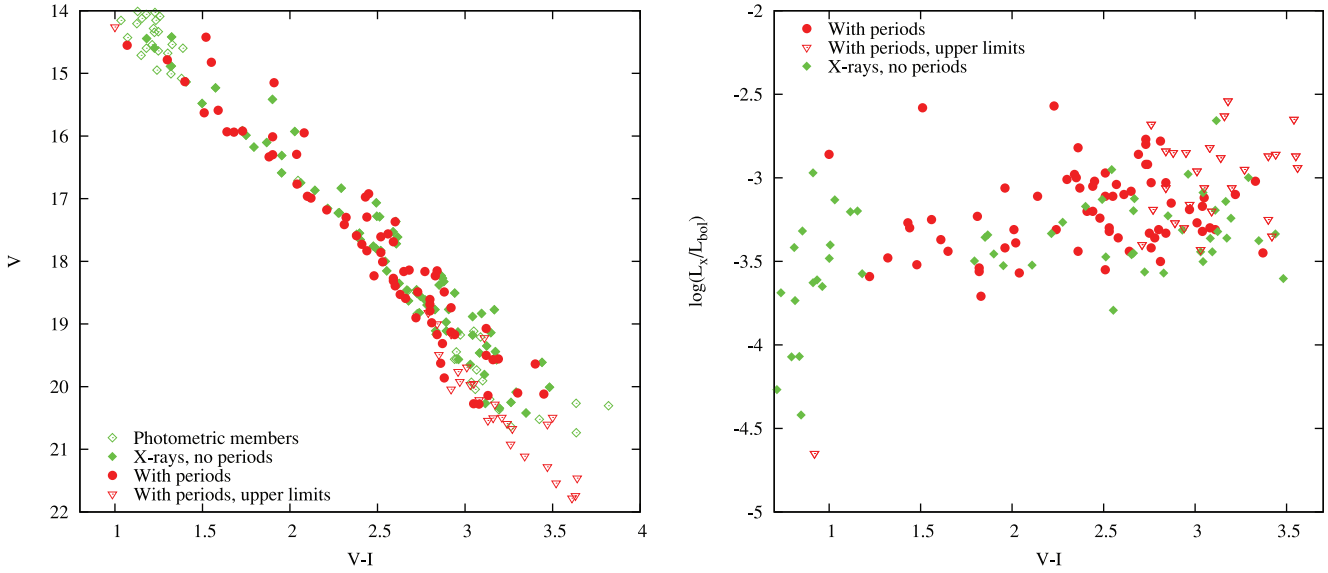

Figure 2. (a) A colour–magnitude diagram in NGC 2547 showing low-mass stars with rotation periods (from Irwin et al. 2008) that have significant X-ray detections (solid circles); stars with rotation periods, that are in the *XMM–Newton* field of view, but have only upper limits to their X-ray activity (open triangles); additional photometric candidate members of NGC 2547 (from Naylor et al. 2002) that are in the *XMM–Newton* field of view (open diamonds); and those additional photometric candidates that are detected in X-rays (filled diamonds). (b) X-ray activity, expressed as $\log L_X/L_{bol}$, as a function of colour. We compare the X-ray activity (and 3σ upper limits to X-ray activity) for stars in NGC 2547 with known rotation periods (from Irwin et al. 2008) to the X-ray activity of detected photometric members of NGC 2547 (from Naylor et al. 2002) that have no known rotation period. Almost all photometric candidate members of NGC 2547 are X-ray detected for $V - I < 2.8$ (see text), so we argue that the members with known rotation periods represent a reasonably unbiased sample with regard to X-ray activity and that the spread of activity at a given colour is less than an order of magnitude for $V - I > 1.2$.

detected and very likely to be genuine NGC 2547 members (see Jeffries et al. 2006 for a detailed discussion). Only for stars with $V - I < 1.5$ and $V - I > 2.8$ are there a significant number of candidates without X-ray detections. For the former, these are likely to be contaminating giants among the photometrically selected members, but the latter are more likely to be genuine cluster members that become too faint for detection at very low luminosities (see below), as indeed are many of the Irwin et al. (2008) objects at similar colours.

Fig. 2(b) plots X-ray activity, expressed as $\log L_X/L_{bol}$, versus colour. There is a gradually rising mean activity level as we move from K- through to M-dwarfs. The upper envelope is ill defined due to three very high points that seem well separated from the rest of the distribution. A time-series analysis of these three stars reveals that each was affected by a large flare during the course of the *XMM–Newton* observation. The lower envelope is well defined for $1 < V - I < 3$ and probably represents a true floor to the level of X-ray activity in cool stars at the age of NGC 2547. Although

our NGC 2547 sample is biased by having detected rotation periods, Irwin et al. (2008) argue that there is not a population of more slowly rotating low-mass stars and Fig. 2(b) also shows that photometrically selected members of NGC 2547 *without* rotation periods, and which also have a *XMM–Newton* counterpart, share a similar minimum (and median) level of X-ray activity as a function of colour. This minimum level is not a product of the sensitivity of the X-ray observations, because almost all photometric candidates with $V - I < 2.8$ and which lie in the *XMM–Newton* field of view have been detected (see Fig. 2a).

The important point that emerges from these arguments is that the range of X-ray activity levels in NGC 2547 at a given colour is quite small (less than an order of magnitude) for young K- and M-dwarfs with $V - I < 2.8$. For cooler stars with $V - I > 2.8$, the X-ray observations become progressively incomplete and we can say very little about the range of X-ray activity here.

3.3 Activity versus rotation period and Rossby number

3.3.1 The dependence of activity on the rotation period

Fig. 3 shows the dependence of activity (L_X/L_{bol}) on the rotation period, considering here only those stars in NGC 2547 with rotation periods given by Irwin et al. (2008). For the purposes of later discussion, we have categorized the stars according to their estimated masses: $0.55 < M/M_\odot < 0.95\,M_\odot$ (roughly corresponding to K-stars, blue circles); $0.35 < M/M_\odot < 0.55$ (corresponding to M0-M3 stars, red crosses); and $M < 0.35\,M_\odot$ (corresponding to stars cooler than M3, black open circles). The masses were estimated from the luminosities of the stars and a 35-Myr isochrone from the evolutionary models of Siess et al. (2000). The bolometric luminosities of our sample were calculated using the corrected, intrinsic V magnitudes, the bolometric corrections described in Section 2.3 and an assumed distance to NGC 2547 of 400 pc (e.g. Mayne & Naylor 2008).

The choice of the mass division at $0.55\,M_\odot$ is to isolate K-dwarfs from the cooler M-dwarfs and at $0.35\,M_\odot$ to mark the approximate transition to a fully convective star (Siess et al. 2000). More importantly, the latter division marks the lowest mass at which our sample can be considered complete, in the sense that X-ray upper limits begin to occur in stars of lower mass. The lowest luminosity stars in the sample have masses of $\simeq 0.1\,M_\odot$.

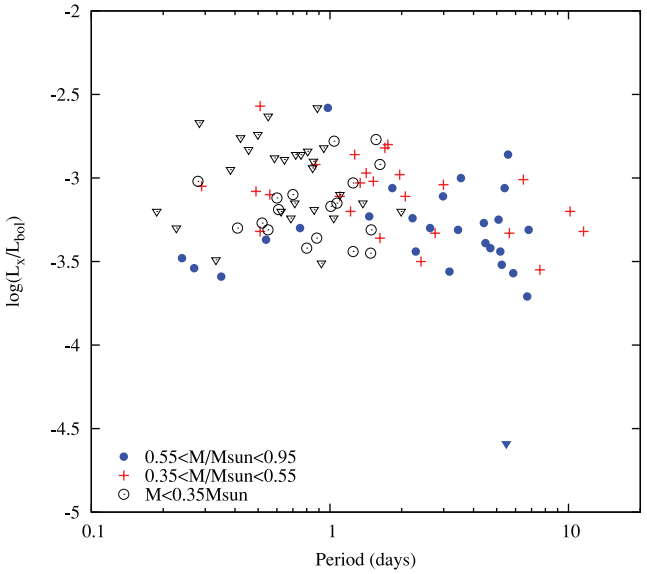

Figure 3. X-ray activity as a function of the rotation period for periodic objects in Irwin et al. (2008) that are in the *XMM–Newton* field of view. The sample has been split according to mass (estimated from the luminosity, see text); detections are denoted with symbols as shown in the plot and upper limits are shown with downward pointing triangles.

Fig. 3 shows that X-rays have been detected from K- and M-dwarfs with periods ranging from 0.2 to 10 d. Most of the upper limits occur for stars with short periods. Given the possibility of a correlation between X-ray activity and rotation, this at first seems surprising. The reason is that most of the lowest luminosity (and hence lowest mass) objects in the Irwin et al. (2008) catalogue have short rotation periods. As the ratio L_X/L_{bol} is close to constant in this sample, this means that many short-period objects have low bolometric *and* X-ray luminosities and are thus harder to detect.

There is a very shallow decline in X-ray activity towards longer periods. As we will show when considering the Rossby numbers for these stars, the reason that the longer period stars do not show much lower X-ray activity is that most of them still have small Rossby numbers and are in the regime where saturated activity levels are expected.

There is some evidence that the very shortest period stars might have lower activity corresponding to 'supersaturation'. This is primarily based on a group of three very low mass stars with $P < 0.4$ d and only upper limits to their X-ray activity and a similar group of three K-stars ($M > 0.55\,M_\odot$) where $L_X/L_{bol} \simeq 10^{-3.5}$.

Any correlations, trends or threshold periods may be confused or blurred by the inclusion of a range of spectral types/convection zone depths within the sample plotted in Fig. 3. It was exactly this issue, which led previous authors to consider the use of the Rossby number as a proxy for magnetic dynamo efficiency (e.g. Noyes et al. 1984; Dobson & Radick 1989; Pizzolato et al. 2003).

3.3.2 Rossby numbers

The use of Rossby number raises a problem when dealing with M-dwarfs. The widely used semi-empirical formula of Noyes et al. (1984) predicts convective turnover time, $\log \tau_c$, as a function of the $B - V$ colour. This relationship is poorly defined for $B - V > 1$ and has no constraining data in the M-dwarf regime. Theoretically, little work has been done on turnover times at very low masses. Gilliland (1986) calculated that the turnover time at the base of the convection zone increases with decreasing T_{eff} and mass along the main sequence. These models are limited to stars $\geq 0.5\,M_\odot$, corresponding to $T_{eff} \geq 3500$ K on the main sequence. $\log \tau_c$ is roughly linearly dependent on $\log T_{eff}$ and increases from about 1.2 (when τ_c is expressed in days) at $T_{eff} = 5800$ K to about 1.85 at 3500 K. Similar calculations, with similar results (except for arbitrary scaling factors), have been presented more recently by Kim & Demarque (1996), Ventura et al. (1998) and Landin, Mendes & Vaz (2010). Ventura et al. (1998) attempted to extend the calculation into the fully convective region, predicting that the convective turnover time would continue to increase. A complication here is that the M-dwarfs of NGC 2547 are not on the main sequence. Gilliland (1986), Kim & Demarque (1996) and Landin et al. (2010) predict that τ_c is about 50 per cent larger for stars of $0.5\,M_\odot$ at an age of $\sim$30 Myr on the PMS.

An alternative approach has been to empirically determine τ_c by demanding that activity indicators (chromospheric or coronal) satisfy a single scaling law with Rossby number, irrespective of stellar mass (e.g. Noyes et al. 1984; Stępień 1994). The most recent work has focused on L_X/L_{bol} as an activity indicator. Using

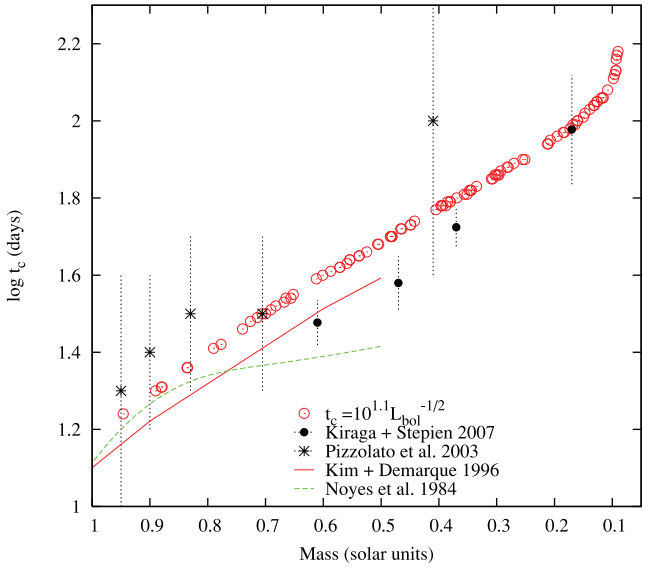

Figure 4. Convective turnover time as a function of stellar mass. The open circles show the turnover times adopted for the NGC 2547 sample, calculated according to $\tau_c \propto L_{bol}^{-1/2}$ (see text), compared with empirical calibrations from Noyes et al. (1984), Pizzolato et al. (2003) and Kiraga & Stępień (2007), and a scaled theoretical 200-Myr isochrone from Kim & Demarque (1996). The masses for the NGC 2547 stars were estimated from their luminosities (see text).

slow- and fast-rotating stars, Pizzolato et al. (2003) showed that τ_c needs to increase rapidly with decreasing mass in order to simultaneously explain L_X/L_{bol} in G-, K- and M-dwarfs, and they find $\log \tau_c > 2$ for $M < 0.5\,M_\odot$. Similar work by Kiraga & Stępień (2007) concentrated on slowly rotating M-dwarfs, finding their empirical $\log \tau_c$ increased from 1.48 at $M \simeq 0.6\,M_\odot$ to 1.98 at $M \simeq 0.2\,M_\odot$. An interesting insight was provided by Pizzolato et al. (2003), who noted that the mass dependence of the turnover time is closely reproduced by assuming that $\tau_c \propto L_{bol}^{-1/2}$. In what follows, we adopt this scaling and hence a Rossby number given by

$$\log N_R = \log P - 1.1 + 0.5 \log L_{bol}/L_\odot \,. \quad (3)$$

The turnover time has been anchored, such that $\log \tau_c = 1.1$ for a solar luminosity star, following the convention adopted by Noyes et al. (1984) and Pizzolato et al. (2003).

In Fig. 4, we compare the τ_c values calculated for our sample as a function of mass, with the theoretical and empirical relationships discussed above. Overall, our τ_c values lie a little below (but not significantly) the Pizzolato et al. (2003) calibration and marginally above the values determined by Kiraga & Stępień (2007) and a theoretical 200-Myr isochrone from Kim & Demarque (1996).[1] From the discussion by these latter authors and their fig. 3, it is clear that any discrepancy between theory and data could be explained by the younger age of NGC 2547. Stars with $M < 1.0\,M_\odot$ are still approaching the main sequence at 30–40 Myr, their τ_c values are still falling and one would expect them to have larger τ_c than for a 200-Myr isochrone or indeed M-dwarf field stars. Unfortunately, Kim & Demarque (1996) did not provide τ_c isochrones at these younger ages. The semi-empirical relationship between τ_c and mass proposed by Noyes et al. (1984) is also shown. As discussed above, this has little or no constraining data below about $0.7\,M_\odot$ and our adopted turnover times in this regime are much larger.

We conclude that our adopted τ_c values and hence Rossby numbers are quite consistent with previous work, although systematic uncertainties at the level of ∼0.2 dex must be present when comparing stars at $M < 0.5\,M_\odot$ with solar mass stars. Tables 1 and 2 include our calculated convective turnover times and Rossby numbers.

3.3.3 *The dependence of activity on Rossby number*

Fig. 5 shows the dependence of L_X/L_{bol} on Rossby number. Dashed loci indicate the approximate divisions between the unsaturated, saturated and supersaturated regimes found from data for G- and K-stars (see Randich 1998; Pizzolato et al. 2003 and Section 4). There is some evidence that the K-stars in our sample ($M > 0.55\,M_\odot$, blue circles) are following the pattern seen in other young clusters. Most of the K-dwarfs appear to have a saturated level of magnetic activity, although we do not clearly see any fall in activity levels at the largest Rossby numbers in our sample. There are three K-dwarfs with $L_X/L_{bol} \simeq 10^{-3.5}$ at $\log N_R < -1.8$, which may be examples of supersaturated stars, and whilst there are also some with similar activity levels at higher Rossby numbers, it is clear that the K-dwarfs with the lowest Rossby numbers are less active than their equivalents in the M-dwarf subsample. The five K-dwarfs with $\log N_R < -1.7$ have a mean $\log L_X/L_{bol} = -3.46 \pm 0.11$ (standard deviation), while the seven M-dwarfs (with $M > 0.35\,M_\odot$) at similar Rossby numbers have a mean $\log L_X/L_{bol} = -3.02 \pm 0.21$.

In the M-dwarf data for NGC 2547 ($M < 0.55\,M_\odot$, red crosses and open circles), there is no decline in activity at large Rossby numbers. This is probably due to a lack of targets with long enough periods to populate the unsaturated regime ($\log N_R > -0.8$, Stauffer et al. 1997). However, there is no doubt that an unsaturated coronal activity regime does exist for field M-dwarfs with long rotation periods (see Kiraga & Stępień 2007 and Section 4).

The lack of obvious supersaturation among the M-dwarfs is more significant. The phenomenon is claimed to begin in G- and K-dwarfs

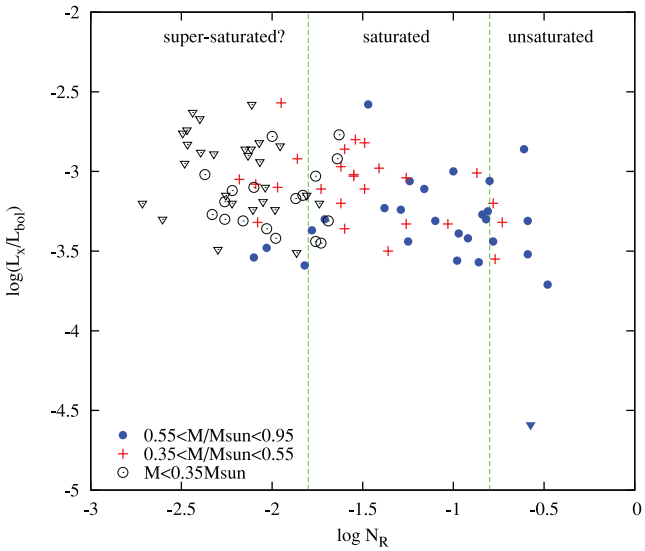

Figure 5. X-ray activity as a function of Rossby number. The sample is divided by mass and shown with symbols as in Fig. 3. The dashed lines indicate divisions between unsaturated, saturated and supersaturated coronal activity defined in the literature for G- and K-stars (see Section 3.3.3).

[1] The τ_c values from Kim & Demarque (1996) were multiplied by 0.31 to anchor them at $\log \tau_c = 1.1$ for a solar mass star.

with $\log N_R \leq -1.8$ (Patten & Simon 1996; Stauffer et al. 1997; Randich 1998) and there are plenty of stars in our sample with much smaller Rossby numbers than this, mostly among the lowest-mass M-dwarfs. A complication here is that the cited papers used relationships in Noyes et al. (1984) to calculate τ_c. However, Fig. 4 shows that Rossby numbers estimated for G- and K-dwarfs ($M > 0.55\,M_\odot$) using the Noyes et al. (1984) formulae would be $\leq$0.2 dex larger than those calculated in this paper for a star of similar mass, so the conclusion is robust.

It is possible that supersaturation begins in the M-dwarfs of NGC 2547 at very low Rossby numbers, say, $\log N_R < -2.3$, but this is only indicated by three upper limits. James et al. (2000) also claimed tentative evidence of supersaturation in their collected sample of field and cluster M-dwarfs. Their claim was based on two stars, VXR47 and VXR60b in IC 2391, which have $(V-I)_0 = 1.7$ and 2.06, respectively, and according to their luminosities would both be classed as late K-dwarfs ($M > 0.55\,M_\odot$) with $\log N_R \simeq -2$ in our classification scheme.

Our conclusion from the NGC 2547 sample is that if supersaturation does occur in M-dwarfs, then it occurs at Rossby numbers that become (in the lowest-mass stars) at least a factor of 3 lower than in supersaturated G- and K-dwarfs.

4 COMBINATION WITH OTHER DATA SETS

The NGC 2547 data suggest that supersaturation does not occur at a single critical Rossby number, irrespective of spectral type (see Fig. 5). Instead, it seems more plausible that supersaturation may occur below some critical period ($\leq$0.4 d, see Fig. 3). This interpretation is hampered by relatively few targets with very short rotation periods and also few targets of higher mass, where the very different convective turnover times would result in quite different Rossby numbers at the same rotation period. To increase our statistics and to make a better comparison with a larger sample of higher mass stars, we combined our data set with published data for stars with known rotation periods in young open clusters and the field. The main sources of the comparison data are catalogues of X-ray activity in field M-dwarfs by Kiraga & Stępień (2007) and in field and cluster dwarfs by Pizzolato et al. (2003). We have also used the recent catalogue of rotation periods in Hartman et al. (2010, see below) to add many new stars from the young Pleiades cluster to the rotation–activity relationship. This large sample covers a range of ages: NGC 2547 at 35 Myr (Jeffries & Oliveira 2005); IC 2391 and IC 2602 at $\simeq$50 Myr (Barrado y Navascués, Stauffer & Jayawardhana 2004); Alpha Per at $\simeq$90 Myr (Stauffer et al. 1999); Pleiades at $\simeq$125 Myr (Stauffer, Schultz & Kirkpatrick 1998); Hyades at $\simeq$625 Myr (Perryman et al. 1998); and field stars that have ages from tens of Myr to many Gyr.

There are important issues to address regarding the completeness of comparison samples. For NGC 2547, we started with stars of known rotation period and determined their X-ray activity level or upper limits to their X-ray activity, if they could not be detected. Almost all stars were detected down to about $0.35\,M_\odot$ (spectral type M3) and there were a mixture of detections and upper limits at lower masses. The samples of stars with known X-ray activity and rotation period found in the literature have been generated in a different way. Generally, field star samples have been compiled by matching objects with known rotation periods to X-ray sources in the *ROSAT* All-Sky Survey (RASS, Voges et al. 1999). In clusters, the data are mostly from *ROSAT* pointed observations, from which detected X-ray sources were matched with known cluster members. The problem is, especially when searching for evidence of supersaturation, that we must be sure that the X-ray observations were sensitive enough to have detected examples of supersaturated stars (say with $L_X/L_{bol} \leq 10^{-3.5}$). This difficulty is exacerbated for active M-dwarfs, because they frequently flare, so there is a possibility that what has been reported in the literature is an X-ray bright tail, disguising a hidden population of undetected, supersaturated M-dwarfs.

For field stars at a given V magnitude, and for a given X-ray flux detection threshold, the corresponding L_X/L_{bol} detection threshold becomes smaller in cooler stars, because the magnitude of the V-band bolometric correction increases. The catalogue of M-dwarfs with rotation periods compiled by Kiraga & Stępień (2007) was taken from optical samples with $V < 12.5$ and correlated with *ROSAT* data, mainly from the RASS. The flux sensitivity of the RASS varies with ecliptic latitude, but the minimum detectable count rate over most of the sky is $\simeq$0.015 count s^{-1}. For a typical coronal spectrum, and neglecting interstellar absorption for nearby stars, this equates to a flux sensitivity of 10^{-13} erg cm^{-2} s^{-1} (e.g. Hünsch et al. 1999). If we consider an M0 dwarf with $V = 12.5$, this flux detection limit corresponds to $L_X/L_{bol} \simeq 1.3 \times 10^{-4}$ and is even lower for cooler M-dwarfs. Hence, the Kiraga & Stępień field M-dwarf sample was easily capable of identifying supersaturation. Similarly, the faintest field M-dwarfs in the Pizzolato et al. (2003) compilation have $V \sim 11$ and would easily be detected at supersaturated activity levels in the RASS. There are thus no completeness problems for the comparison samples of field dwarfs.

In a cluster, all stars are at the same distance, so a given X-ray-flux detection limit corresponds to an L_X threshold, and cooler stars with smaller L_{bol} are harder to detect at a given L_X/L_{bol}. In most clusters observed by *ROSAT*, and included in the Pizzolato et al. compilation, the sensitivity was sufficient to detect all G- and K-dwarfs, but only a fraction of M-dwarf members were detected (e.g. Stauffer et al. 1994; Randich et al. 1995, IC 2602; Randich et al. 1996, Alpha Per; Micela et al. 1999, the Pleiades). Furthermore, in some clusters (e.g. IC 2391 – Patten & Simon 1996), members were *identified* on the basis of their X-ray detection and their rotation periods were determined afterwards. In these circumstances, it is likely that the M-dwarfs identified in the cluster observations will have mean activity levels biased upwards by selection effects and there would be little chance of identifying supersaturation even if it were present. The cluster M-dwarfs from Pizzolato et al. (2003) are therefore clearly identified in what follows.

In the case of the Pleiades, these difficulties were circumvented by replacing those Pleiades stars in Pizzolato et al. (2003) with a sample constructed by cross-correlating the Hartman et al. (2010) catalogue of rotation periods for G-, K- and M-dwarfs with the *ROSAT* source catalogues (including upper limits) of Micela et al. (1999) and Stauffer et al. (1994) (in that order of precedence where sources were detected in both). In this way we constructed a Pleiades catalogue of 111 stars detected by *ROSAT*, with rotation periods $0.26 \leq P \leq 9.04$ d and masses (see below) of $0.33 < M/M_\odot < 0.95$, along with 18 stars with $0.35 \leq P \leq 9.41$ d and $0.18 < M/M_\odot < 0.95$ that have only X-ray upper limits. The Hartman et al. (2010) catalogue has a relatively bright magnitude limit and hence few very low mass stars. Nevertheless, there were 38 detections and 10 upper limits for objects classed here as M-dwarfs ($M < 0.55\,M_\odot$).

Masses were calculated for the field and cluster dwarfs using bolometric luminosities listed in the source papers and the $Z = 0.02$ Siess et al. (2000) models with (i) a 1 Gyr age for the field stars and stars in the Hyades; (ii) a 100 Myr age for stars in the Alpha

Per and Pleiades clusters; and (iii) a 50 Myr age for stars in the IC 2391 and IC 2602 clusters. Rossby numbers were calculated using equation (3). L_X/L_{bol} values were taken from Pizzolato et al. (2003) and Kiraga & Stępień (2007), or from Stauffer et al. (1994) and Micela et al. (1999) for the Pleiades. The X-ray fluxes in these papers are quoted in the 0.1–2.4 keV *ROSAT* passband. The spectral model adopted for NGC 2547 in Section 3.3 predicts that a flux in the 0.1–2.4 keV band would only be 6 per cent higher than the 0.3–3 keV fluxes reported in Table 1. This difference is small enough to be neglected in our comparisons.

The combined data are shown in Fig. 6, where correlations between activity and period, and activity and Rossby number are investigated. The stars have been split into three mass ranges (the same subsets as in Section 3.3) to see whether period or Rossby number is the best parameter with which to determine X-ray-activity levels across a broad range of masses and convection zone depths. The number of stars taken from each of the clusters and the field in each of the three mass ranges is: NGC 2547 (45 for $<0.35\,M_\odot$, 25 for $0.35 < M/M_\odot < 0.55$, 26 for $0.55 < M/M_\odot < 0.95$); IC 2391/2602 (0, 3, 24); Alpha Per (0, 2, 29); Pleiades (10, 38, 71); Hyades (0, 1, 8); and Field (8, 27, 44)

The additional data, particularly more fast rotating K-dwarfs and slow-rotating M-dwarfs, clarifies a number of issues:

(i) The left-hand panels of Fig. 6 show that both slowly rotating K- and M-dwarfs have a decreasing level of coronal activity at long periods. However, the rotation period alone appears to be a poor indicator of X-ray activity for slowly rotating stars. K-dwarfs and M-dwarfs follow different rotation–activity relationships at long periods – compare the M-dwarfs with the (red) solid locus, which approximately indicates the relationship followed by the K-dwarfs. The rotation period at which saturation sets in may be longer for lower mass stars.

(ii) The addition of further fast-rotating K-dwarfs, mainly from other young clusters, clearly demonstrates a supersaturation effect at $P < 0.3$ d. The evidence for supersaturation in M-dwarfs is not convincing: there are two upper limits (from NGC 2547 and also present in Fig. 3) that may suggest supersaturation at $P \simeq 0.2$ d in the lowest-mass stars. However, the few additional short-period M-dwarfs from the comparison samples show no indication of supersaturation down to periods of 0.25 d.

(iii) The Rossby number (or at least the Rossby number found from the convective turnover times that we have calculated) unifies the low-activity side of the rotation–activity correlation (in the right-hand panels of Fig. 6). The Rossby number is capable of predicting the level of X-ray activity with a modest scatter and applies to a wide range of masses and convection zone depths, including some stars, which are fully or nearly fully convective. Coronal saturation occurs, within the limitations of the small number statistics for the lowest-mass stars, at a similar range of Rossby numbers ($-1.8 < \log N_R < -0.8$) for all low-mass stars and at a similar value of L_X/L_{bol}.

(iv) For $\log N_R < -1.8$, the Rossby number does less well in predicting what happens to the coronal activity. Whilst there is evidence that some G- and K-dwarfs supersaturate at $\log N_R < -1.8$, there is a large scatter. There is no evidence for declining activity at low Rossby numbers among the M-dwarfs, unless the two upper limits at $\log N_R < -2.5$ in NGC 2547 mark the beginning of supersaturation at much lower Rossby numbers. Comparing the left-hand and right-hand panels of Fig. 6, it may be that, for fast-rotating stars, the rotation period is the better parameter to determine when and if supersaturation occurs.

(v) None of these conclusions is affected by the inclusion or otherwise of cluster M-dwarfs from Pizzolato et al. (2003) that may be subject to an upward selection bias.

(vi) There are three K-dwarfs (one detection – HII 1095 and two upper limits – HII 370 and HII 793) in the Pleiades sample, with P in the range 0.87–0.94 d, which have anomalously low X-ray activity. We do not believe these are examples of coronal supersaturation, but more likely they are stars where the period found by Hartman et al. (2010) is a 1-d alias of a true longer period.

5 DISCUSSION

A summary of the findings of Sections 3 and 4 would be that X-ray activity rises with decreasing Rossby number, reaches a saturation plateau at a critical Rossby number ($\log N_R \simeq -0.8$) that is approximately independent of the stellar mass and then becomes supersaturated at a smaller Rossby number in a way that *is* dependent on the stellar mass – either in the sense that supersaturation does not occur at all in low-mass M-dwarfs or if it does, it occurs at much lower Rossby numbers than for K-dwarfs. The Rossby number is the parameter of choice to describe the occurrence of saturation and the decline of activity at slower rotation rates, but the rotation period may be a better parameter for predicting the occurrence of supersaturation at $P \sim 0.3$ d in K-dwarfs and perhaps $P \sim 0.2$ d in lower mass stars.

There are a number of ideas that could explain the progression from the unsaturated to satuarated to supersaturated coronal regimes: (i) feedback effects in the dynamo itself may manifest themselves at high rotation rates. The increasing magnetic field could suppress differential rotation and the capacity to regenerate poloidal magnetic field (e.g. Robinson & Durney 1982; Kitchatinov & Rüdiger 1993; Rempel 2006); (ii) the photosphere may become entirely filled with equipartition fields (e.g. Reiners, Basri & Browning 2009). This leads to saturation of magnetic activity indicators in the corona and chromosphere. At faster rotation rates, it is possible that the magnetic field emerges in a more restricted way (e.g. constrained to higher latitudes – Solanki et al. 1997; Stępień et al. 2001), reducing the filling factor again and leading to supersaturation; and (iii) at high rotation rates, centrifugal forces could cause a rise in pressure in the summits of magnetic loops, which then break open or become radiatively unstable, reducing the emitting coronal volume and emission measure (Jardine & Unruh 1999).

The results from NGC 2547 and Fig. 6 favour an explanation for saturation in terms of saturation of the dynamo or magnetic filling factor, rather than a simple dependence on the rotation rate. The coronal activity of low-mass and very low mass M-dwarfs in the right-hand panels of Fig. 6 is well described by the same relationship between activity and Rossby number as the higher mass K-dwarfs, at least for $\log N_R > -1.8$. The Rossby number at which coronal activity saturates is also broadly similar across a wide range of masses. These facts suggest that X-ray activity levels depend primarily on Rossby number, which is a key parameter describing the efficiency of a magnetic dynamo (Durney & Robinson 1982; Robinson & Durney 1982). Supporting evidence for an explanation involving saturation of magnetic flux generation comes from direct measurements of magnetic flux in fast-rotating M-dwarfs (Saar 1991; Reiners et al. 2009) and from chromospheric magnetic activity indicators, which also show saturation at Rossby numbers of $\simeq$0.1 (Cardini & Cassatella 2007; Marsden, Carter & Donati 2009). A caveat to this conclusion is that the convective turnover times and hence Rossby numbers of the lowest-mass stars in our

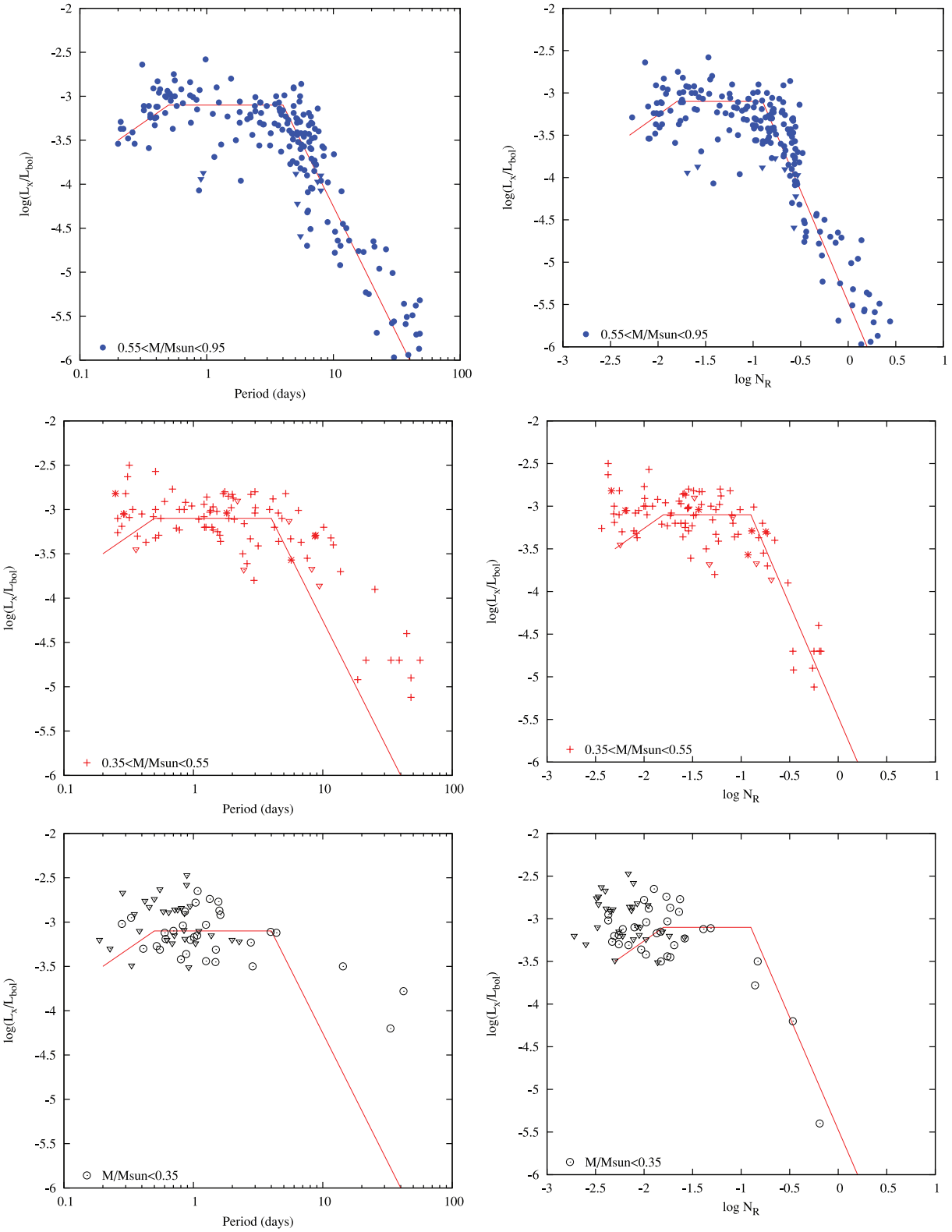

Figure 6. X-ray activity as a function of the rotation period (left-hand column) or as a function of Rossby number (right-hand column) for low-mass stars in NGC 2547 and for literature compilations of cluster and field dwarfs as explained in the text. The plots are separated according to the estimated masses of the stars (top panels: K-stars with $0.55 < M/\mathrm{M}_{\odot} < 0.95$; middle panels: M-stars with $0.35 < M/\mathrm{M}_{\odot} < 0.55$; bottom panels: M-stars with $M < 0.35\,\mathrm{M}_{\odot}$, the symbols are those used in Fig. 3). The loci in each plot are by-eye trends identified in the K-stars and then repeated in the subsequent plots to highlight differences with stellar mass. Cluster M-dwarfs from Pizzolato et al. (2003) may be subject to an upward bias (see text) and are marked with asterisks.

sample are uncertain. In fact, the semi-empirical scaling of $\tau_c \propto L_{bol}^{-1/2}$ was *designed* to minimize the scatter at large Rossby numbers (Pizzolato et al. 2003). Clearly, better theoretical calculations of τ_c are desirable for $M < 0.5\,M_\odot$.

The phenomenon of supersaturation does not seem to be well described by Rossby numbers calculated using similar τ_c estimates. Some G- and K-dwarfs show supersaturation at $\log N_R \simeq -1.8$, but using the same τ_c values that tidy up the low-activity side of Fig. 6 implies that M-dwarfs do not supersaturate, unless at $\log N_R \simeq -2.5$. This suggests that supersaturation may not be intrinsic to the dynamo mechanism, a point of view supported by the lack of supersaturation in the chromospheric emission from very rapidly rotating G- and K-dwarfs (Marsden et al. 2009). It is worth noting that the lack of supersaturation in M-dwarfs is probably not related to any fundamental change in dynamo action, such as a switch from an interface dynamo to a distributed dynamo as the convection zone deepens. There are sufficient M-dwarfs in Fig. 6 with $M > 0.35\,M_\odot$, which should still have radiative cores (Siess et al. 2000), to demonstrate that they also show no signs of supersaturation at the Rossby numbers of supersaturated G- and K-dwarfs.

Stępień et al. (2001) put forward a hypothesis that a latitudinal dependence of the heating flux at the base of the convection zone is caused by the polar dependence of the local gravity in rapid rotators. This could result in strong poleward updrafts in the convection zone that sweep magnetic flux tubes to higher latitudes, leaving an equatorial band that is free from magnetically active regions, hence reducing the filling factor of magnetically active regions in the photosphere, chromosphere and corona. In this model, supersaturation occurs when the ratio of the centrifugal acceleration at the surface of the radiative core to the local gravitational acceleration reaches some critical value γ, that is,

$$G M_c R_c^{-2} = \gamma 4\pi^2 R_c P^{-2}, \quad (4)$$

where M_c and R_c are the mass and radius of the radiative core.

Leaving aside the issue of what happens in fully convective stars, we can make the approximation that $M_c R_c^{-3}$ is approximately proportional to the central density, so that the period P_{ss} at which supersaturation would be evident depends on the central density as $P_{ss} \propto \rho_c^{-1/2}$ (assuming that the convection zone rotates as a solid body). The central density as a function of mass is very time-dependent on the PMS. At 35 Myr, a star of $0.3\,M_\odot$ has $\rho_c = 3000\,\mathrm{kg\,m^{-3}}$, while a 0.9-$M_\odot$ star has $\rho_c = 6900\,\mathrm{kg\,m^{-3}}$ (Siess et al. 2000). At 100 Myr, however, the core of the 0.3-$M_\odot$ star is nearly three times denser, while the 0.9-$M_\odot$ star remains almost unchanged. Thanks to the inverse square root dependence on density, however, one would expect supersaturation to occur at quite similar periods in objects with a range of masses and certainly with a variation that is much smaller than if supersaturation occurred at a fixed Rossby number. However, there is no evidence of supersaturation in the chromospheric activity of G- and K-dwarfs, which *are* coronally supersaturated (Marsden et al. 2009), and this argues that a simple restriction of the filling factor due to a polar concentration of the magnetic field is not the solution.

Jardine & Unruh (1999) have shown that dynamo saturation or complete filling by active regions may not be necessary to explain the observed plateau in X-ray activity and its subsequent decline at very fast rotation rates. In their model, centrifugal forces act to strip the outer coronal volume, either because the plasma pressure exceeds what can be contained by closed magnetic loops (see also Ryan et al. 2005) or because the coronal plasma becomes radiatively unstable beyond the Keplerian corotation radius (Collier-Cameron 1988). The reduced coronal volume is initially balanced by a rising coronal density, causing a saturation plateau, but at extreme rotation rates, as more of the corona is forced open, the X-ray emission measure falls (see also Jardine 2004).

We might expect centrifugal effects to become significant in the most rapidly rotating stars and whilst there will clearly be a correlation with Rossby number, there will be an important difference in mass dependence. The key dimensionless parameter in the centrifugal stripping model is α_c, the corotation radius expressed as a multiple of the stellar radius,

$$\alpha_c = \left(\frac{G M_* P^2}{4\pi^2 R_*^3}\right)^{1/3} \propto M_*^{1/3} R_*^{-1} P^{2/3}, \quad (5)$$

where P is the rotation period. Thus, coronal activity should saturate at some small value of α_c and then supersaturate at an even smaller α_c. In the samples considered here, there is a two order of magnitude range in P but a much smaller range in $M_*^{1/3} R_*^{-1}$. Hence, we expect to see saturation and supersaturation occur at short periods corresponding to some critical values of α_c. However, in stars with lower masses and smaller radii, these critical α_c values will be reached at *shorter* periods, such that $P_{ss} \propto M^{-1/2} R^{3/2}$, which in NGC 2547 varies from 0.9 (in solar units) for the most massive stars in our sample to 0.5 in the lowest-mass stars. Hence, supersaturation in the M-dwarfs would occur at shorter periods than for K-dwarfs by a factor approaching 2.

To test these ideas, Fig. 7 shows L_X/L_{bol} as a function of both $\log N_R$ and α_c, with the stars grouped into mass subsets in a similar way to Sections 3 and 4. The stellar radii and masses for the comparison samples were estimated from their luminosities and the Siess et al. (2000) models as described in Sections 3 and 4.

The α_c parameter, like the rotation period, is a poor predictor of what happens to X-ray activity in the slowly-rotating and low-activity regimes. Saturated levels of coronal activity are reached for $\alpha_c = 10$–30, dependent on the mass of the star. We interpret this to mean that centrifugal forces have a negligible effect on coronal structures in this regime. For large values of α_c and concomitantly large values of $\log N_R$, we suppose that coronal activity is determined by the efficiency of the magnetic dynamo, hence explaining the reasonably small scatter within the shaded area of the left-hand panel of Fig. 7. On the other hand, supersaturation seems to be achieved when $\alpha_c \lesssim 2.5$, and the modest scatter within the shaded area of the right-hand panel of Fig. 7, compared to that for $\log N_R < -1.8$ in the left-hand panel, suggests that centrifugal effects may start to control the level of X-ray emission somewhere between this value and $\alpha_c \sim 10$.

In this model, it now becomes clear that the reason we have no clear evidence for supersaturation in M-dwarfs is that they are not spinning fast enough for their coronae to be affected by centrifugal forces. There are only two very low mass M-dwarfs in our sample (from NGC 2547) with $\alpha_c < 2.5$ and they do have upper limits to their activity that could be indicative of supersaturation.

If the corona is limited at some small multiple of the corotation radius, it implies that X-ray-emitting coronal structures exist up to this extent above the stellar surface. The arguments for and against the presence of such extended coronal structures are summarized by Güdel (2004). Perhaps the best-supporting evidence comes from the 'slingshot prominences' observed to occur around many rapidly rotating stars, which often form at or outside the corotation radius (e.g. Collier-Cameron & Robinson 1989; Jeffries 1993; Barnes et al. 1998), which may signal the action of the centrifugal stripping process.

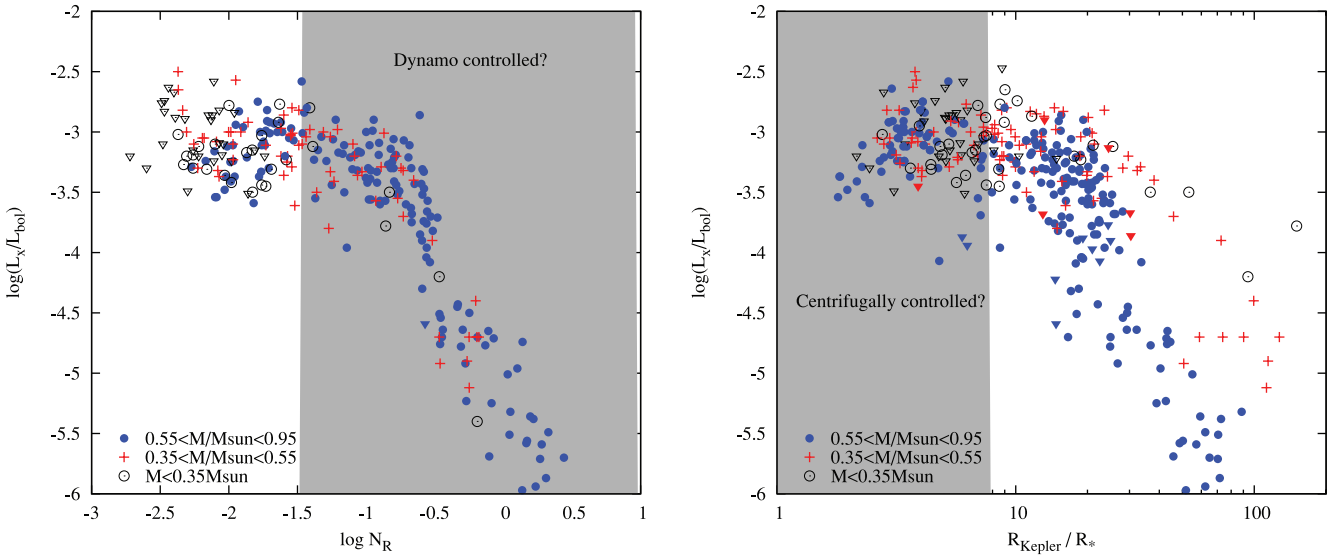

Figure 7. X-ray activity as a function of Rossby number (left-hand panel) and Keplerian corotation radius (right-hand panel, expressed as a fraction of the stellar radius). The sample is divided by mass as in Fig. 3. The shaded regions indicate the approximate regimes in which we hypothesize that the coronal activity is controlled by magnetic dynamo efficiency (at large Rossby number in the left-hand plot) or by centrifugal effects (for small Keplerian corotation radii in the right-hand plot).

6 SUMMARY

We have determined the level of X-ray activity (in terms of L_X/L_{bol}) for a sample of low-mass K- and M-dwarfs with rotation periods of 0.2–10 d, in the young ($\simeq$35 Myr) open cluster NGC 2547. A deep *XMM–Newton* observation is able to detect X-rays from almost all stars with $M \geq 0.35\,M_\odot$ and provides detections or upper limits for many more with lower masses. Most targets exhibit saturated levels of X-ray activity ($L_X/L_{bol} \simeq 10^{-3}$), but a few of the most rapidly rotating showed evidence of lower, 'supersaturated' activity. The evidence for supersaturation in M-dwarfs with $M < 0.55\,M_\odot$ is weak, limited to three objects with short periods and very small Rossby numbers, which have 3σ upper limits to their coronal activity of $L_X/L_{bol} \leq 10^{-3.3}$–$10^{-3.4}$.

These data were combined with X-ray measurements of fast-rotating low-mass stars in the field and from other young clusters, and the results were considered in terms of stellar rotation period and in terms of the Rossby number, which is thought to be diagnostic of magnetic dynamo efficiency. The main result is that while coronal saturation appears to occur below a threshold Rossby number, $\log N_R \lesssim -0.8$, independent of stellar mass, there is evidence that supersaturation does not occur at a fixed Rossby number. Supersaturation in the lowest-mass M-dwarfs occurs, if at all, at Rossby numbers that are at least three times smaller than those for which supersaturation is observed to occur in G- and K-dwarfs; there is no evidence for supersaturation in M-dwarfs with $\log N_R > -2.3$. Instead, it appears that a rotation period <0.3 d is a more accurate predictor of when supersaturation commences and there are only a few M-dwarfs rotating at these periods in our sample.

A caveat to this result is that our calculated Rossby numbers rely on rather uncertain semi-empirical values of the convective turnover time. However, these turnover times do unify the slowly-rotating side of the rotation–activity relation in the sense that the use of Rossby numbers significantly reduces the scatter in this relationship and predicts a common threshold Rossby number for coronal saturation.

These phenomena can be interpreted within a framework where coronal saturation occurs due to saturation of the dynamo itself at a critical Rossby number, or perhaps due to complete filling of the surface by magnetically active regions. Coronal supersaturation is probably not an intrinsic property of the dynamo, but instead associated with topological changes in the coronal magnetic field with fast rotation rates. The observations favour the centrifugal stripping scenario of Jardine & Unruh (1999) and Jardine (2004), in which the reduction of the available coronal volume due to instabilities induced by centrifugal forces leads to a drop in X-ray emission as the Keplerian corotation radius moves in towards the surface of the star.

If centrifugal stripping is the correct explanation for supersaturation, then M-dwarfs should supersaturate at shorter periods than K-dwarfs, by factors of up to ~2. The data analysed here are sparse but consistent with this idea. Determining the X-ray emission from a small sample of rapidly rotating ($P < 0.25$ d) M-dwarfs would resolve this issue. The centrifugal stripping idea may also explain the positive correlation between X-ray activity and rotation period seen in very young PMS stars by Stassun et al. (2004) and Preibisch et al. (2005). It could be that the fastest-rotating young PMS stars are centrifugally stripped, whilst those of slower rotation are merely saturated. Investigating this in detail faces formidable observational and theoretical difficulties, not least the estimation of the intrinsic, non-accretion-related X-ray emission, individual absorption column densities for stars and the determination of PMS stellar radii, masses and convective turnover times.

ACKNOWLEDGMENTS

Based on observations obtained with *XMM–Newton*, an ESA science mission with instruments and contributions directly funded by ESA Member States and the NASA. RJJ acknowledges the receipt of a Science and Technology Facilities Council postgraduate studentship.

REFERENCES

Audard M., Güdel M., Drake J. J., Kashyap V. L., 2000, ApJ, 541, 396
Barnes J. R., Collier-Cameron A., Unruh Y. C., Donati J. F., Hussain G. A. J., 1998, MNRAS, 299, 904
Barrado y Navascués D., Stauffer J. R., Jayawardhana R., 2004, ApJ, 614, 386
Bohlin R. C., Savage B. D., Drake J. F., 1978, ApJ, 224, 132
Briggs K., Pye J. P., 2003, MNRAS, 345, 714
Cardini D., Cassatella A., 2007, ApJ, 666, 393
Carrera F. J. et al., 2007, A&A, 469, 27
Clariá J. J., 1982, A&AS, 47, 323
Collier-Cameron A., 1988, MNRAS, 233, 235
Collier-Cameron A. C., Robinson R. D., 1989, MNRAS, 238, 657
Cruddace R. G., Dupree A. K., 1984, ApJ, 277, 263
Dahm S. E., Simon T., Proszkow E. M., Patten B. M., 2007, AJ, 134, 999
D'Antona F., Mazzitelli I., 1997, Mem. Soc. Astron. It., 68, 807
Dobson A. K., Radick R. R., 1989, ApJ, 344, 907
Doyle J. G., 1996, A&A, 307, L45
Durney B. R., Robinson R. D., 1982, ApJ, 253, 290
Gagné M., Caillault J. P., Stauffer J. R., 1995, ApJ, 450, 217
García-Alvarez D., Drake J. J., Kashyap V. L., Lin L., Ball B., 2008, ApJ, 679, 1509
Gilliland R. L., 1986, ApJ, 300, 339
Guainazzi M., 2010, Technical Report XMM-SOC-CAL-TN-0018, EPIC status of calibration and data analysis, Version 2.9. XMM-Newton SOC
Güdel M., 2004, ARA&A, 12, 71
Hartman J. D., Bakos G. Á., Kovács G., Noyes R. W., 2010, MNRAS, 408, 475
Hünsch M., Schmitt J. H. M. M., Sterzik M. F., Voges W., 1999, A&AS, 135, 319
Irwin J., Hodgkin S., Aigrain S., Bouvier J., Hebb L., Moraux E., 2008, MNRAS, 383, 1588
James D. J., Jardine M. M., Jeffries R. D., Randich S., Collier Cameron A., Ferreira M., 2000, MNRAS, 318, 1217
Jardine M., 2004, A&A, 414, L5
Jardine M., Unruh Y. C., 1999, A&A, 346, 883
Jeffries R. D., 1993, MNRAS, 262, 369
Jeffries R. D., Oliveira J. M., 2005, MNRAS, 358, 13
Jeffries R. D., Tolley A. J., 1998, MNRAS, 300, 331
Jeffries R. D., Naylor T., Devey C. R., Totten E. J., 2004, MNRAS, 351, 1401
Jeffries R. D., Evans P. A., Pye J. P., Briggs K. R., 2006, MNRAS, 367, 781
Kim Y.-C., Demarque P., 1996, ApJ, 457, 340
Kiraga M., Stępień K., 2007, Acta Astron., 57, 149
Kitchatinov L. L., Rüdiger G., 1993, A&A, 276, 96
Kitchatinov L. L., Rüdiger G., Küker M., 1994, A&A, 292, 125
Kraft R. P., Burrows D. N., Nousek J. A., 1991, ApJ, 374, 344
Landin N. R., Mendes L. T. S., Vaz L. P. R., 2010, A&A, 510, A46
Leggett S. K., Allard F., Berriman G., Dahn C. C., Hauschildt P. H., 1996, ApJS, 104, 117
Lyra W., Moitinho A., van der Bliek N. S., Alves J., 2006, A&A, 453, 101
Mangeney A., Praderie F., 1984, A&A, 130, 143
Marino A., Micela G., Peres G., Sciortino S., 2003, A&A, 406, 629
Marsden S. C., Carter B. D., Donati J., 2009, MNRAS, 399, 888
Mayne N. J., Naylor T., 2008, MNRAS, 386, 261
Mewe R., Kaastra J. S., Leidahl D. A., 1995, Technical report, The HEASARC Journal, Legacy Volume 6. Goddard Space Flight Center
Micela G. et al., 1999, A&A, 341, 751
Naylor T., Jeffries R. D., 2006, MNRAS, 373, 1251
Naylor T., Totten E. J., Jeffries R. D., Pozzo M., Devey C. R., Thompson S. A., 2002, MNRAS, 335, 291
Noyes R. W., Hartmann L., Baliunas S. L., Duncan D. K., Vaughan A. H., 1984, ApJ, 279, 763
Pallavicini R., Golub L., Rosner R., Vaiana G. S., Ayres T., Linsky J. L., 1981, ApJ, 248, 279
Park T., Kashyap V. L., Siemiginowska A., van Dyk D. A., Zezas A., Heinke C., Wargelin B. J., 2006, ApJ, 652, 610
Patten B. M., Simon T., 1996, ApJS, 106, 489
Perryman M. A. C. et al., 1998, A&A, 331, 81
Pizzolato N., Maggio A., Micela G., Sciortino S., Ventura P., 2003, A&A, 397, 147
Preibisch T. et al., 2005, ApJS, 160, 401
Prosser C. F., Randich S., Stauffer J. R., Schmitt J. H. M. M., Simon T., 1996, AJ, 112, 1570
Randich S., 1998, in Donahue R. A., Bookbinder J. A., eds, ASP Conf. Ser. Vol. 154, Supersaturation in X-ray Emission of Cluster Stars. Astron. Soc. Pac., San Francisco, p. 501
Randich S., Schmitt J. H. M. M., Prosser C. F., Stauffer J. R., 1995, A&A, 300, 134
Randich S., Schmitt J. H. M. M., Prosser C. F., Stauffer J. R., 1996, A&A, 305, 785
Reiners A., Basri G., Browning M., 2009, ApJ, 692, 538
Rempel M., 2006, ApJ, 647, 662
Robinson R. D., Durney B. R., 1982, A&A, 108, 322
Ryan R. D., Neukirch T., Jardine M., 2005, A&A, 433, 323
Saar S. H., 1991, in Tuominen I., Moss D., Rüdiger G., eds, The Sun and Cool Stars: Activity, Magnetism, Dynamos Recent Advances in the Observation and Analysis of Stellar Magnetic Fields. Springer-Verlag, Berlin, p. 389
Saxton R. D., 2003, Technical Report XMM-SOC-CAL-TN-0023, A statistical evaluation of the EPIC flux calibration, Version 2.0. XMM-Newton SOC
Siess L., Dufour E., Forestini M., 2000, A&A, 358, 593
Solanki S. K., Motamen S., Keppens R., 1997, A&A, 324, 943
Stassun K. G., Ardila D. R., Barsony M., Basri G., Mathieu R. D., 2004, AJ, 127, 3537
Stauffer J. R., Caillault J. P., Gagné M., Prosser C. F., Hartmann L. W., 1994, ApJS, 91, 625
Stauffer J. R., Hartmann L. W., Prosser C. F., Randich S., Balachandran S., Patten B. M., Simon T., Giampapa M., 1997, ApJ, 479, 776
Stauffer J. R., Schultz G., Kirkpatrick J. D., 1998, ApJ, 499, L199
Stauffer J. R. et al., 1999, ApJ, 527, 219
Stępień K., 1994, A&A, 292, 191
Stępień K., Schmitt J. H. M. M., Voges W., 2001, A&A, 370, 157
Strüder L. et al., 2001, A&A, 365, L18
Telleschi A., Gudel M., Briggs K., Audard M., Ness J. U., Skinner S. L., 2005, ApJ, 622, 653
Turner M. J. L. et al., 2001, A&A, 365, L27
Ventura P., Zeppieri A., Mazzitelli I., D'Antona F., 1998, A&A, 331, 1011
Vilhu O., Walter F. M., 1987, ApJ, 321, 958
Voges W. et al., 1999, A&A, 349, 389

SUPPORTING INFORMATION

Additional Supporting Information may be found in the online version of this article:

Table 1. X-ray detections of sources in the Irwin et al. (2008) catalogue of NGC 2547 members with rotation periods.
Table 2. The properties of stars from the Irwin et al. (2008) catalogue that have known rotation periods but were not detected within the *XMM–Newton* field.

Please note: Wiley-Blackwell are not responsible for the content or functionality of any supporting materials supplied by the authors. Any queries (other than missing material) should be directed to the corresponding author for the article.

This paper has been typeset from a TEX/LATEX file prepared by the author.